

## Reducing both CAPEX and OPEX thanks to CFD at Gabal-el-Asfar WWTP: hydraulic optimization of flow distribution to clarifiers and sedimentation tanks

Núria Margarit Bel\*, César Retana Pastor, Jorge J. Malfeito Sánchez

*Acciona Agua S.A.U., Parc de Negocis Mas Blau II, Avda. de les Garrigues, 22 – 2ª Planta, 08820 El Prat de Llobregat, Barcelona, Spain  
Tel. +34 93 335 15 00; Fax +34 93 336 60 21; e-mail: nuria.margarit.bel@acciona.com*

Received 25 March 2015; Accepted 13 June 2016

### ABSTRACT

Acciona Agua is currently building Gabal-el-Asfar wastewater treatment plant (WWTP) which is designed to process waste water from El Cairo, Egypt. As a main advantage, computational fluid dynamic tools (CFD) can evaluate hydraulics in 3 dimensions (3D) previous to any construction. Commercial software utilized by the R&D department of Acciona Agua was used to predict and then optimize flow performance for diverse plant elements early in the engineering process, during the detail design period. On one hand, one element susceptible to be enhanced while reducing construction capital costs was identified. On the other hand, equipment that could present hydraulic performance issues during operation was also recognized. A novel approach using CFD techniques could help solve foreseen issues in both cases. Executed simulations allowed depth minimization of the distribution chamber to the final clarifiers, while maintaining flow supply variation within  $\pm 5\%$  of the expected value. Also, simulations anticipated flow performance of the distribution chamber to the primary sedimentation tanks. A corrective action such as placement of baffle columns helped flow homogenization and induced proper water flow distribution to each sedimentation tank, with  $\pm 1.5\%$  deviation from the average. As a conclusion, CFD proved to be an effective tool that provided vital information for hydraulic optimization and consequent cost reduction of Gabal-el-Asfar WWTP.

*Keywords:* CFD; Wastewater; Optimization

### 1. Introduction

At Gabal El-Asfar WWTP (GEA), the distribution chambers designed to deliver appropriate water flow to the primary sedimentation tanks and to the final clarifiers respectively, present different shapes and profiles.

From one side, there was a need to corroborate equal flow supply from the squared distribution chamber to the primary sedimentation tanks at GEA. A proper hydraulic study could help optimize its operating conditions and positively cut OPEX. From the other side, there was an opportunity to reduce construction depth of the circular distribution chamber to the final clarifiers, while main-

taining proper flow distribution. This could then represent CAPEX savings during GEA civil works.

Therefore, and previous to construction, computational fluid dynamic tools (CFD) were used to evaluate flow performance in 3-dimensions (3D) of the aforementioned chambers. CFD main advantage is that it helps understand equipment 3D flow performance before any construction is started. CFD is a low-cost, high speed modeling technique, which avoids other evaluation systems (such as laboratory or field tests) that may be difficult or not possible to perform [1,2]. Numerical solutions provide crucial information that can optimize shapes and sizes prior to civil works and plant commissioning [3,4]. CFD simulations are reliable as long as underlying principles are recognized and properly utilized [5,6].

\*Corresponding author.

### 1.1. Distribution to primary sedimentation tanks

GEA equipment dimensions and operating conditions for the distribution chambers to the primary sedimentation tanks are detailed below.

Mass flow rate to the distribution chamber upstream of the primary sedimentation tanks was considered on the worst case scenario, that is, when treating  $8.356 \text{ m}^3 \text{ s}^{-1}$  of water. Flow enters the chamber through a 3000 mm diameter concrete pipe which is connected to the bottom of one of the four walls of the square plant view, and then, must be distributed among six different outlets by overflow. The overflow wall is situated 12.29 m from the bottom of the tank and water gets split between 6 equally distributed compartments, two on each of the remaining walls, which will convey the received flow to the primary sedimentation tanks.

Anticipating that such profile could generate bad flow distribution among the six outlets, a corrective action based on company's know-how was conceived [7,8]. Results for Atotonilco WWTP CFD study recommended the installation of baffle columns inside the chamber. Both Fig. 1 and Fig. 2 show three triangular 3-m height columns specifically designed to homogenize incoming flow and properly distribute water. CFD simulations were performed first using the base geometry, that is, without baffles. Then, and after results were analyzed, the model was replicated for the baffled geometry and the new simulation results were compared to the un-baffled version.

Once the above presented geometry was converted to a hydraulic CFD model (Figs. 1, 2), the final result for the baffled case was as shown in Fig. 3, where the inlet is colored blue and the outlets are in red. Each exit compartment was numbered from 1 to 6 counterclockwise to assist in further representations.

fled case was as shown in Fig. 3, where the inlet is colored blue and the outlets are in red. Each exit compartment was numbered from 1 to 6 counterclockwise to assist in further representations.

### 1.2. Circular distribution chamber to clarifiers

GEA mass flow rate to the circular distribution chamber upstream of the final clarifiers was considered for the worst case scenario, that is, when treating  $11.37 \text{ m}^3 \text{ s}^{-1}$  of water.

The aforementioned water flow rate enters the chamber through a 3000 mm diameter pipe which is connected to the bottom of the system by a cubic-shaped cavity (4.5 m per side). From there, four walls transform such square section into a circular one, 12.5 m in diameter. The overflow wall is situated 9.93 m from the bottom of the tank and water gets split between 6 equally distributed compartments, each one with the corresponding collector that sends the flow to the final clarifiers. When ideally working, the chamber should divide the inlet mass flow to six equal streams of  $1891 \text{ kg s}^{-1}$  each. In case there is a  $\pm 5\%$  deviation, exit flows should fall between  $1797 \text{ kg s}^{-1}$  and  $1986 \text{ kg s}^{-1}$ .

When optimizing the design, the only possible modification to the system lied on the inlet cubic-shaped cavity, which could be reduced 1 m in depth and hence the inlet pipe, could also be raised 1 m. As a consequence, on the new analyzed geometry, the overflow wall was situated 8.83 m from the bottom.

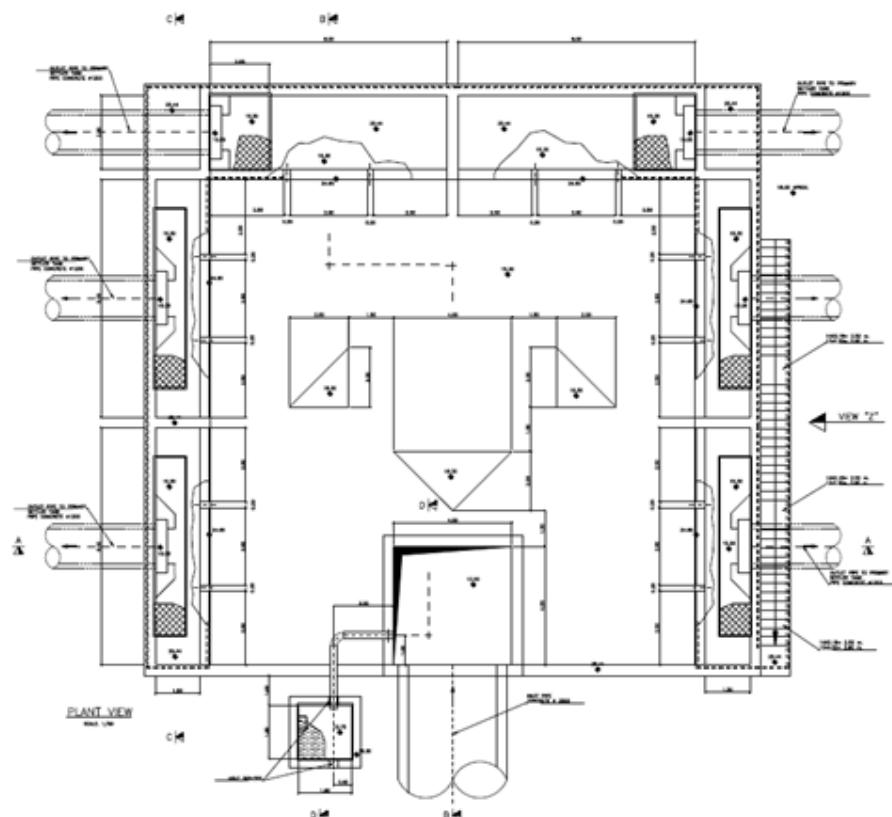


Fig. 1. Distribution chamber of primary sedimentation tanks. Plant view.

Once the chamber geometry was converted to a hydraulic CFD model, the final result was as shown in Fig. 6, where the inlet is colored blue and the outlets are red. Each exit compartment was numbered from 1 to 6 counterclockwise to assist in further representations.

2. Software and methods

Software utilized by the R&D department of Acciona Agua is Ansys Fluent 14.5. All CFD simulations

ran on a dual core 2.8Hz Intel Xeon 64-bit Windows XP workstation.

CFD modeling not only needs geometries to be accurately meshed and cases not to be sensitive to mesh size, but it also needs a series of boundary conditions to properly define the system. Boundary conditions usually correspond to real operating conditions. Nevertheless, in order to simulate a flow model that included the free-surface between the water and the atmosphere, as happens in this equipment, a group of settings had to be considered for both distribution chamber cases:

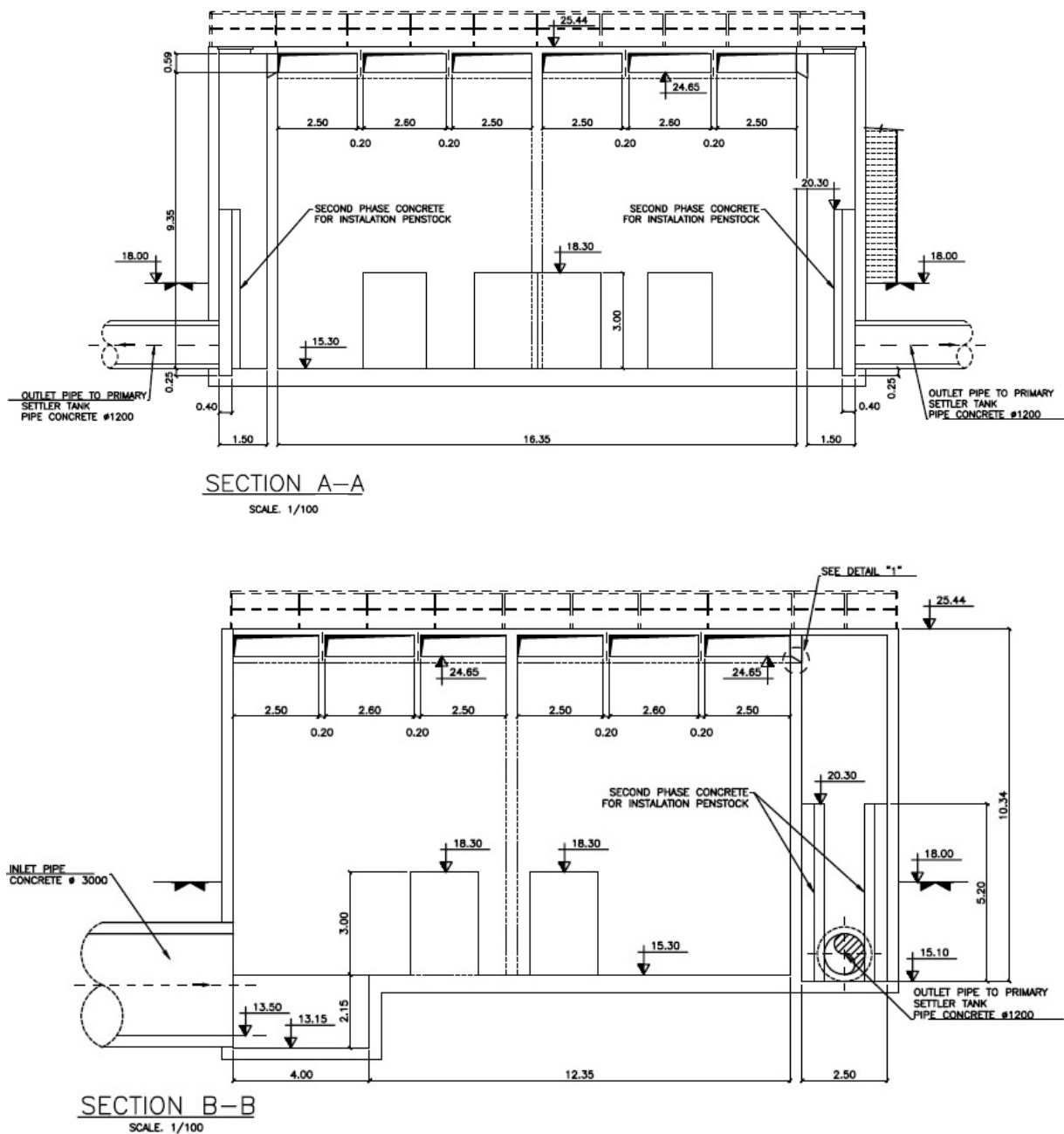


Fig. 2. Distribution chamber of primary sedimentation tanks. Sections.

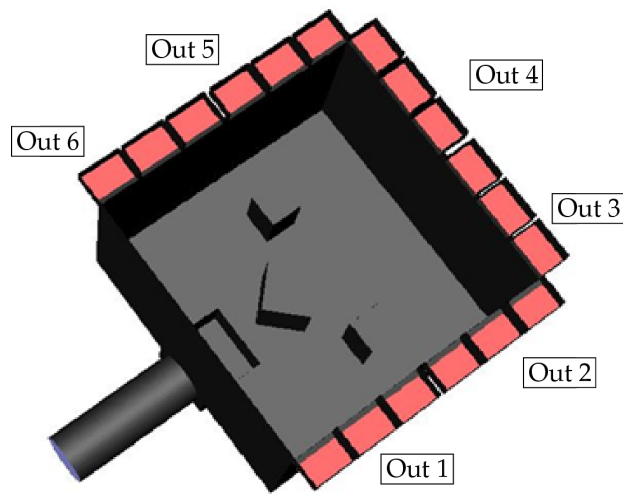


Fig. 3. CFD model for primary sedimentation tank with baffles.

- The numerical models were solved as a VOF (volume of fluid), where both phases, air and water, were simulated.
- All cases were simulated as transitory, that is, the distribution chamber was initially full to the overflow level and on stand-by. At time zero seconds, water started flowing into the system through the inlet pipe. The model then ran for as long simulated time as needed to achieve a pseudo-steady state (in both cases, for approximately 3 min).
- Water distribution to each exit compartment was calculated automatically by mass balance and simulated as open channel.
- Velocity profile at the inlet was considered as perfectly homogeneous. Elbows or other accessories that may affect the flow pattern inside the feed pipe were not considered.

All cases ran using two different sets of meshes, a coarse mesh version of about 1 million cells and a refined meshed version, with x1.5 finer mesh, in order to verify results were not affected by elements size.

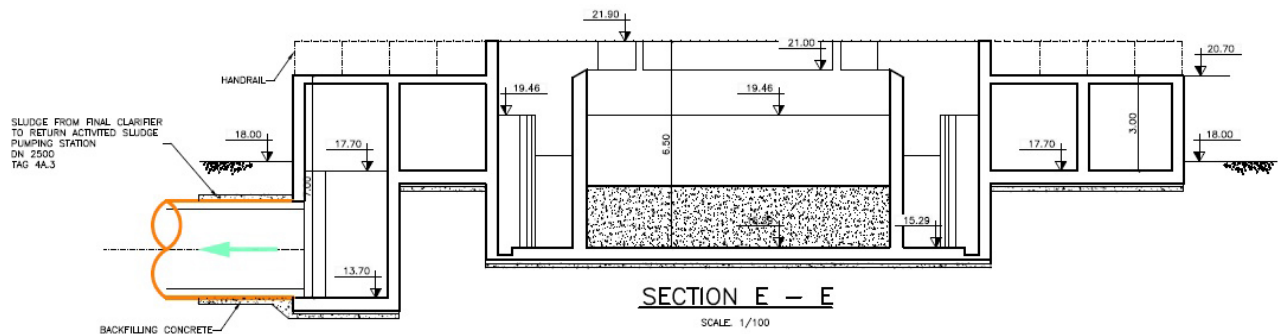


Fig. 4a. Distribution chamber of final clarifiers. Section E-E.

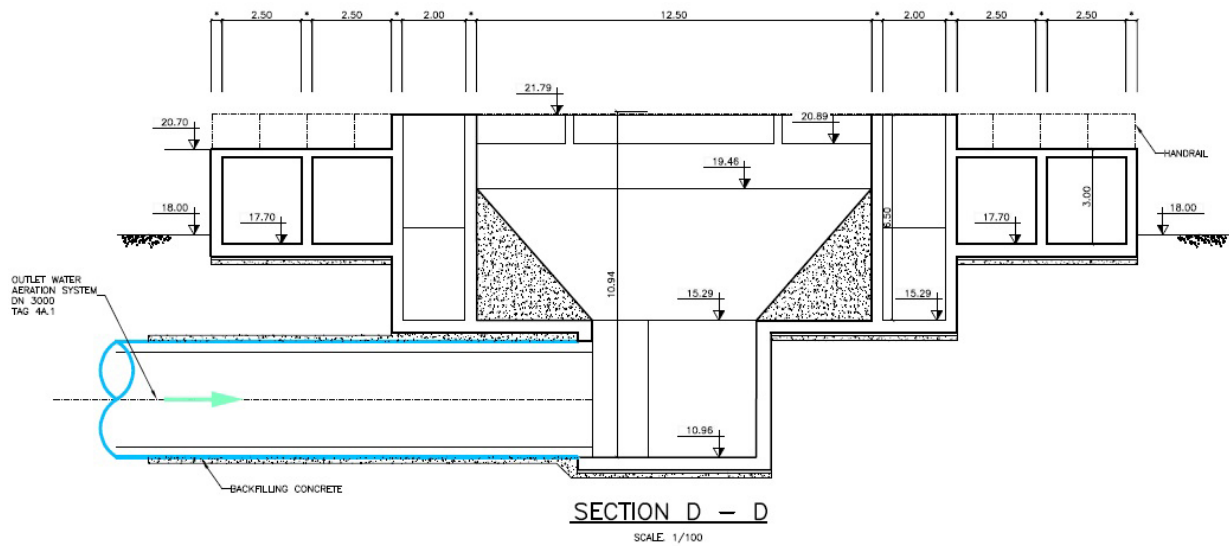


Fig. 4b. Distribution chamber of final clarifiers. Section D-D.

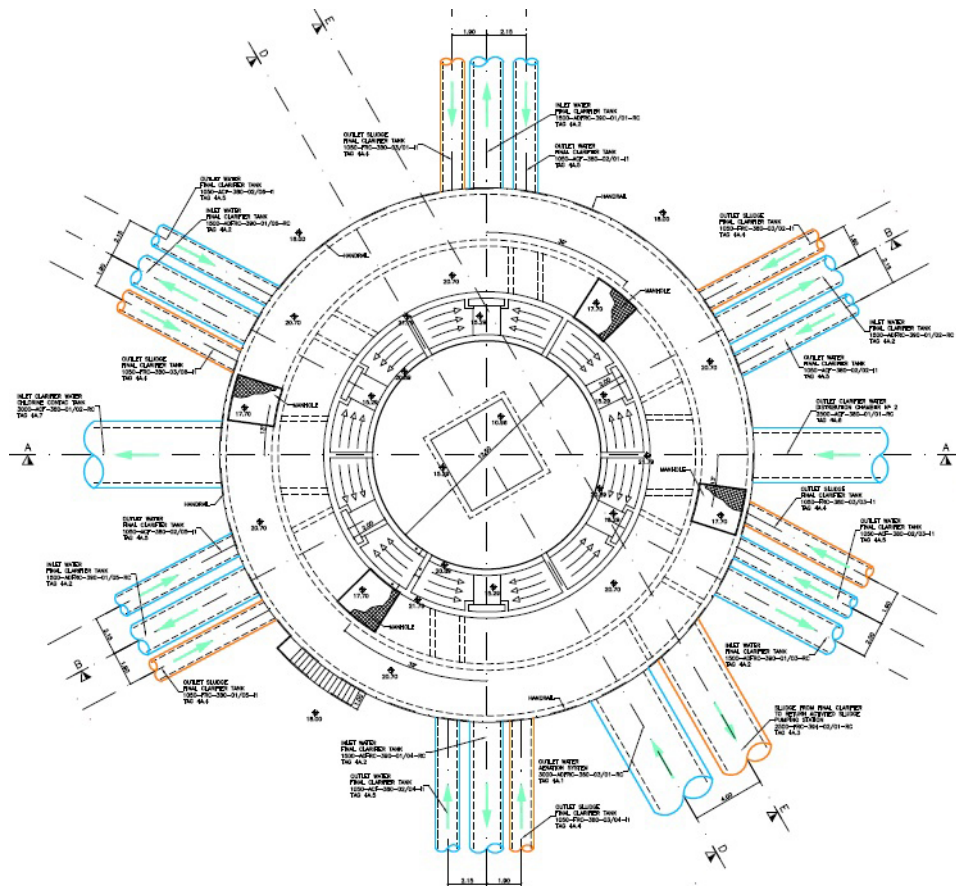


Fig. 5. Distribution chamber of final clarifiers. Plant view.

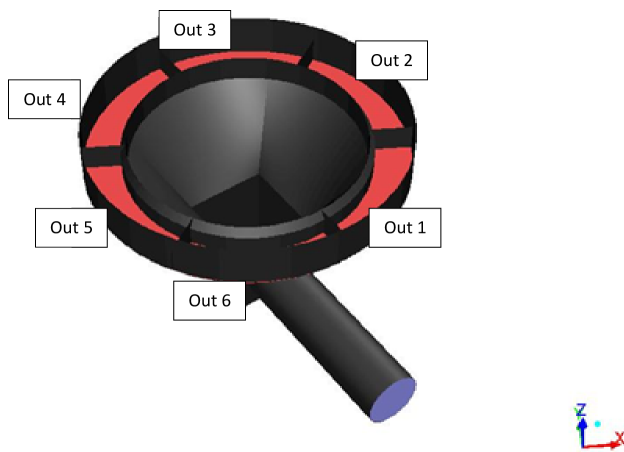


Fig. 6. CFD model for the base geometry of the circular distribution chamber.

All CFD models ran for approximately 200 simulated seconds using 8-processors. Each case needed 7 full days to reach such state.

### 3. CFD results and analysis

#### 3.1. Distribution to primary sedimentation tanks

First, a simulation of the base geometry distribution chamber to the primary sedimentation tanks was run. When depicting velocity profiles on different slices of the model, although it is not totally obvious, one could predict a tendency of the water flow to abandon the chamber through outlets 1 and 6 (see Figs. A.1, A.2 in appendix A). Mass flow was not mainly overflowing through exits 3 and 4 because the incoming jet would bounce on the wall opposite to the inlet, and most of the water would return close to the entrance, then leaving through the nearby exits.

If representing the independent outlet flow rates during 10 s, once the simulation steady state was achieved (200 s), the following table could be generated:

Thus, from Table 1, one could note that not only outlet 1 and 6 received the most water, but there was also an important oscillation in mass flow rate exiting through those outlets. For this reason, a case simulating the same distribution chamber and that included baffle columns to homogenize the flow was next run.

In Appendix A, Fig. A.3–A.5, velocity profiles at different planes, when baffle columns were installed, are presented. This set of images demonstrated the good performance of the baffle columns, which were situated exactly

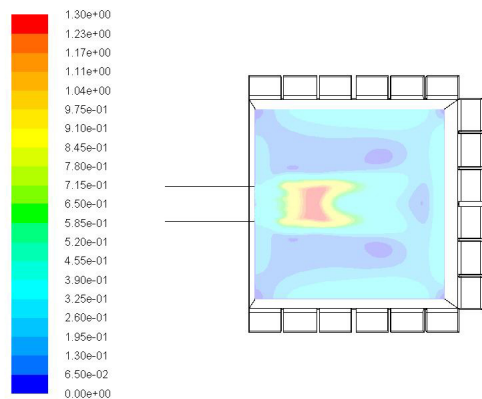


Fig. A.1. Velocity magnitude ( $\text{m s}^{-1}$ ) at 3.5 m from the bottom at 200 s, case without baffles.

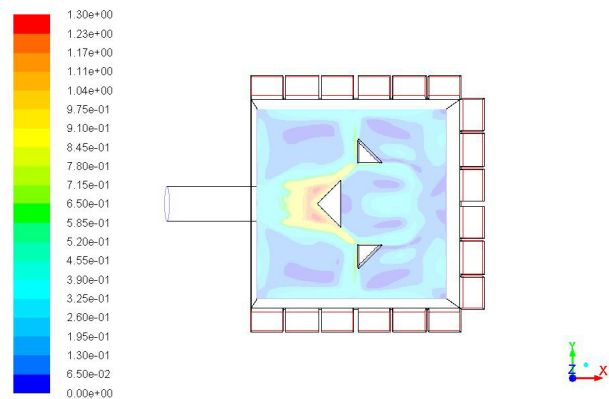


Fig. A.3. Velocity magnitude ( $\text{m s}^{-1}$ ) at 3.5 m from the bottom at 200 s, case with baffles.

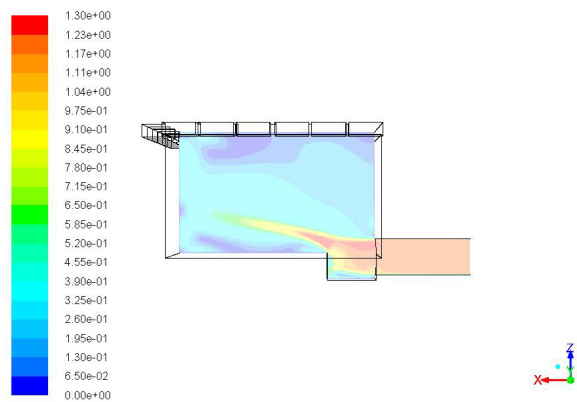


Fig. A.2. Velocity magnitude ( $\text{m s}^{-1}$ ) at center line of inlet pipe at 200 s, case without baffles.

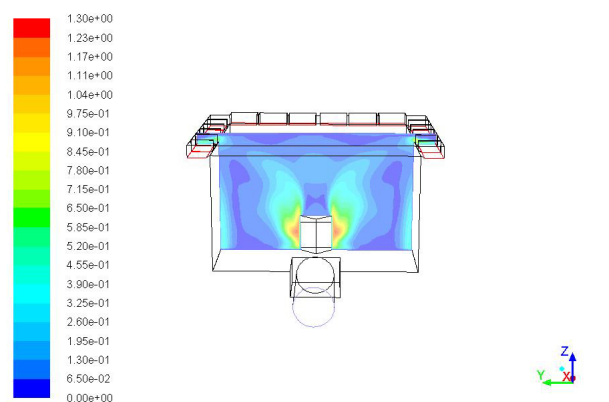


Fig. A.4. Velocity magnitude ( $\text{m s}^{-1}$ ) at 4.5 m from the inlet at 200 s, case with baffles.

Table 1  
Mass flow rate [ $\text{kg s}^{-1}$ ] through each outlet of the distribution chamber to primary sedimentation tanks, with no baffles. Ideal mass flow rate should be  $1365 \text{ kg s}^{-1}$

Outlet number	Minimum flow rate	Maximum flow rate	Deviation from ideal
1	1444	1456	+6.1%
2	1321	1325	-3.1%
3	1323	1329	-2.9%
4	1320	1329	-3.0%
5	1322	1327	-2.9%
6	1436	1465	+6.2%

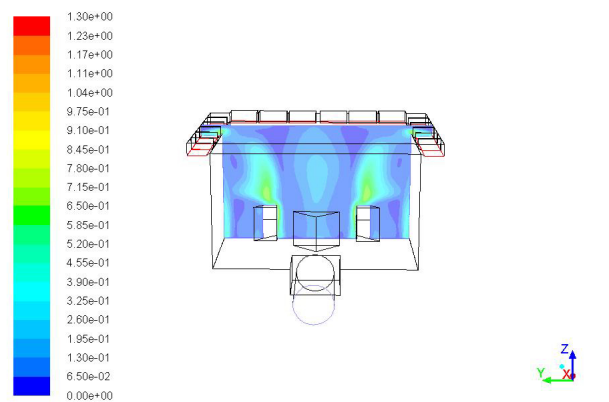


Fig. A.5. Velocity magnitude ( $\text{m s}^{-1}$ ) at 7.5 m from the inlet at 200 s, case with baffles.

at the center of the flow jet and split the fluid mass into equal amounts inside the tank volume.

In this case, when baffles were included in the model, mass flow rates for each outlet produced results as in Table 2.

This time all flow rates fell within less than 1.5% of the expected value. Therefore, no more design iterations were considered necessary to simulate. As a standard procedure, all cases were ran under the same boundary conditions and

settings, but using two different mesh sizes, a coarse one and a finer one. As long as the finer mesh generated the same results as the coarse mesh, simulations were then validated, as it was the case.

Even though results will not be experimentally corroborated until plant commissioning is finished, CFD simulations are endorsed by previous company know-how [8]. A very similar study was performed for Atotonilco wastewa-

Table 2

Mass flow rate [ $\text{kg s}^{-1}$ ] through each outlet of the distribution chamber to primary sedimentation tanks, with baffles. Ideal mass flow rate should be  $1365 \text{ kg s}^{-1}$

Outlet number	Minimum flow rate	Maximum flow rate	Deviation from ideal
1	1375	1386	+1.3%
2	1350	1356	-0.7%
3	1349	1355	-0.6%
4	1350	1356	-0.6%
5	1352	1354	-0.7%
6	1375	1380	+1.1%

ter treatment plant in Mexico, when distribution chambers to biological reactors were analyzed by equivalent numerical methods. In this case, on-site testing of the final design has already been performed and thus, necessary simulation assumptions and their corresponding results have been validated.

Figs. 7, 8 are graphics that depict water mass flow rate leaving through each of the 6 outlets for both simulated distribution chambers around 200 s, once steady state was achieved. A discontinuous red line represents the expected exit water mass flow rate for comparison. Installed baffles were thus proven to help homogenize mass flow distribution, reducing deviation from ideal from an initial 6% in some outlets to less than 1.5% for all of them.

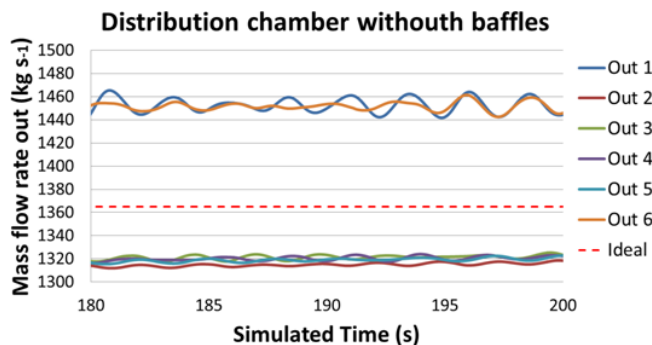


Fig. 7. Mass flow ( $\text{kg s}^{-1}$ ) distribution to the 6 outlets along the simulated time (s) for distribution chamber without baffles.

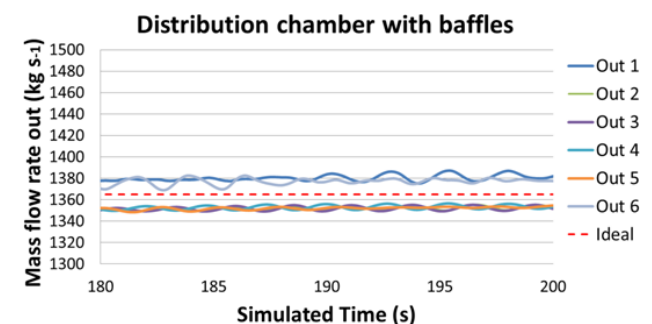


Fig. 8. Mass flow ( $\text{kg s}^{-1}$ ) distribution to the 6 outlets along the simulated time (s) for distribution chamber with baffles.

### 3.2. Circular distribution chamber to clarifiers

When simulating the circular distribution chamber to the final clarifiers, one could expect very homogeneous distribution thanks to its symmetric and round design. But in fact, after the base geometry case was run, results showed otherwise. Again, two CFD models with different mesh sizes were created and run. Both provided equivalent results and thus, used for discussion below.

In Fig. 9, which represents the velocity magnitude at the free-surface, one could already note that some compartments received more water than others, since down-pour velocity was higher for the same area (outlet 5 sees higher velocity than outlet 6). Also, velocity profile on the surface was not completely homogeneous. Horizontal slices of the distribution chamber were next investigated to search for the origin of such heterogeneity (see Fig. B.1–B.3 in appendix B). Then, a tendency of the flow to impact the opposite wall to the inlet was noticed. The fluid bounced back to the sides and, to a lesser extent, reached those compartments further from the entry.

However, when representing mass flow rate evolution with time, as in Fig. 10, all values were very close to the established operating maximums and minimums, set to a 5% deviation in this case. That is, the distribution chamber for this particular case was considered to work properly as long as all distribution deviations were less than 5% (Table 3).

Since the performance of the circular chamber was considered appropriate, an investigation trying to minimize the basin size was carried next. Having 1 m margin at the entry from the bottom, another simulation was run using a new geometry which was 1 m less in depth.

Fig. 11 shows the velocity magnitude at the free-surface for the final state of the simulation of the modified design. One could again note that some compartments received more water than others. Nevertheless, velocity profile on the surface was not equivalent in both models. One geometry differed from the other in flow behavior.

The origin for such differences was sought through velocity profiles representation at diverse but equivalent chamber heights from the bottom. In Fig. B.4–B.6 in appendix B one could mainly distinguish velocity magnitude peaks, which in the modified version were higher in some points near the wall. This could be explained because flow was more concentrated in that area and it did not

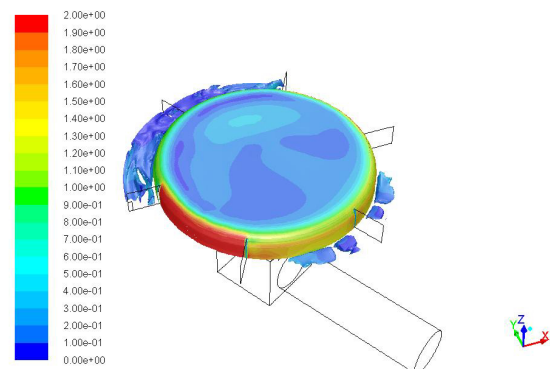


Fig. 9. Velocity magnitude ( $\text{m s}^{-1}$ ) at the water free-surface at 200 s for original depth.

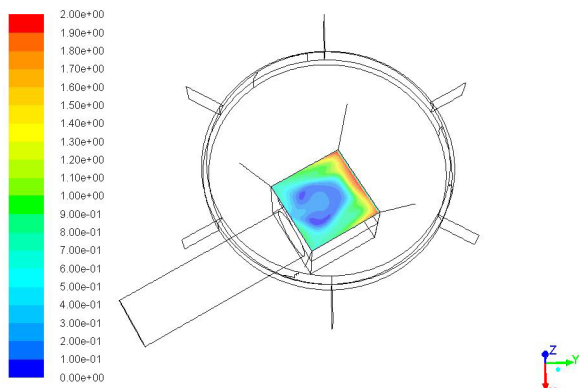


Fig. B.1. Velocity magnitude ( $\text{m s}^{-1}$ ) at 4.3 m from the bottom at 200 s for original depth.

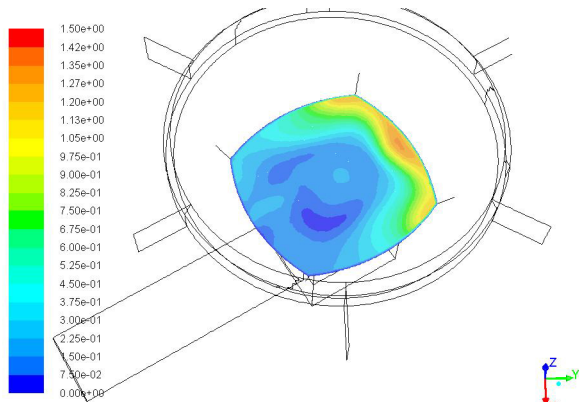


Fig. B.2. Velocity magnitude ( $\text{m s}^{-1}$ ) at 6 m from the bottom at 200 s for original depth.

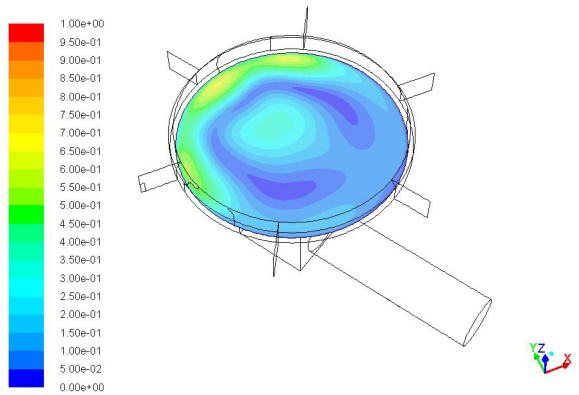


Fig. B.3. Velocity magnitude ( $\text{m s}^{-1}$ ) at 8.5 m from the bottom at 200 s for original depth.

have time to disperse as in the original case, which being deeper, had larger available volume (residence time). This had a direct effect on flow distribution, since mass flow rate to those compartments closer to the inlet (outlet 1 and 6) became smaller.

In general, more flow abandoned the chamber through the back compartments in the modified design than in the original one. However, both models presented similar grades of flow variation, reaching a 5% difference among outlets (Fig. 12 and Table 4).

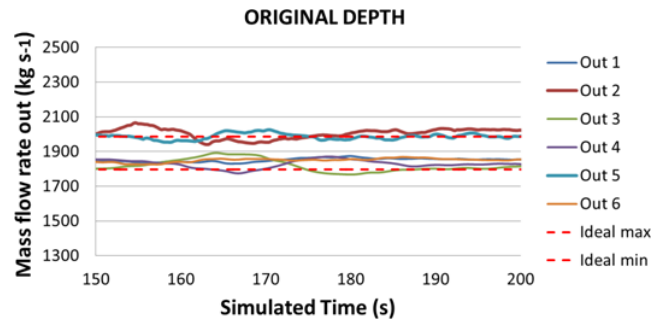


Fig. 10. Mass flow ( $\text{kg s}^{-1}$ ) distribution to the 6 outlets along the simulated time (s).

Table 3

Averaged mass flow rate ( $\text{kg s}^{-1}$ ) at steady state through each simulated outlet and %deviation from the expected or ideal value when original depth is simulated

Outlet	1	2	3	4	5	6
Mass flow ( $\text{kg s}^{-1}$ )	1850	2002	1825	1831	1987	1849
% Deviation	-2.1%	+5.8%	-3.5%	-3.2%	+5.0%	-2.1%

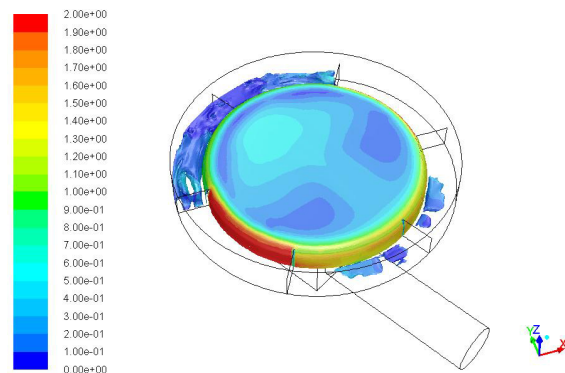


Fig. 11. Velocity magnitude ( $\text{m s}^{-1}$ ) at the water free-surface at 190 s for 1 m-less depth.

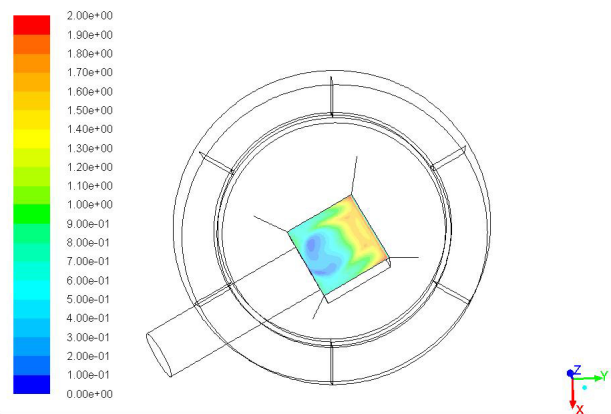


Fig. B.4. Velocity magnitude ( $\text{m s}^{-1}$ ) at 3.3 m from the bottom at 190 s for 1 m-less depth.

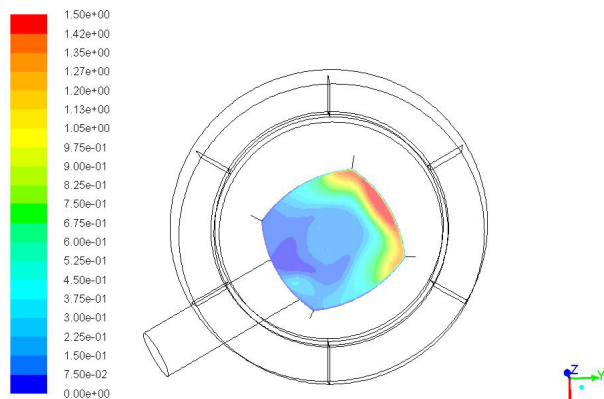


Fig. B.5. Velocity magnitude (m/s) at 5m from the bottom at 190s for 1m-less depth.

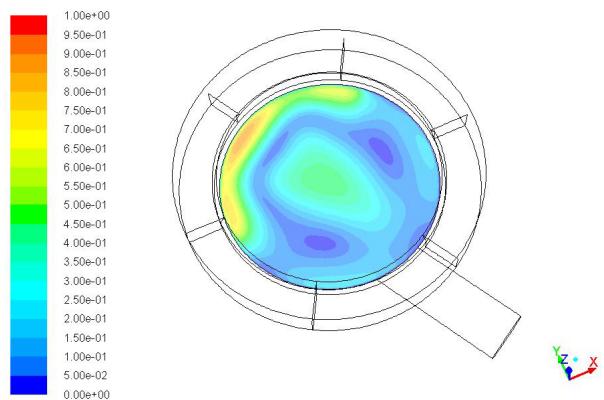


Fig. B.6. Velocity magnitude (m s<sup>-1</sup>) at 7.5 m from the bottom at 190 s for 1 m-less depth.

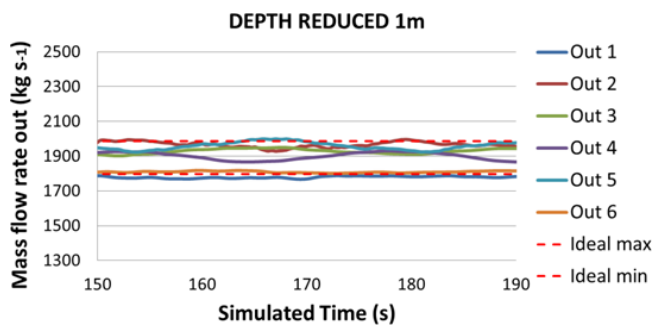


Fig. 12. Mass flow (kg s<sup>-1</sup>) distribution to the 6 outlets along the simulated time (s).

Table 4  
Averaged mass flow rate (kg s<sup>-1</sup>) at steady state through each simulated outlet and % deviation from the expected or ideal value when 1 m-reduced depth is simulated

Outlet	1	2	3	4	5	6
Mass flow (kg s <sup>-1</sup> )	1780	1968	1925	1895	1965	1808
% Deviation	-5.8%	+4.1%	+1.8%	+0.2%	+3.9%	-4.3%

As a final conclusion, although flow behavior of both tested depths appeared different, final effect over flow distribution was equivalent, and thus either configuration could be used for proper performance. In order to reduce civil works expenses, the modified version (less deep) of the circular distribution chamber to the final clarifiers was recommended.

#### 4. Conclusions

Two different elements at Gabal El-Asfar (GEA) wastewater treatment plant were identified as susceptible to hydraulics performance improvement, and thus, operating cost reduction or even civil works savings.

From one side, proper flow distribution to the primary sedimentation tanks at GEA, downstream of the distribution chamber was checked thanks to a 3D CFD model using Ansys Fluent 14.5. Simulation results showed that both lateral exits closer to the inlet received the most flow, exceeding 6% from the expected value. A corrective action was taken, and three column baffles were placed and simulated so the new designed chamber distributed the water mass flow rate to each sedimentation tank with a deviation less than ±1.5%.

On the other side, proper flow distribution to the final clarifiers at GEA was also checked through CFD models with different geometry depths. In general, although flow behavior of both tested depths appeared different, final effect over flow distribution was equivalent, and either configuration could be used for proper performance while maintaining water flow distribution to each clarifier with a deviation of ±5%.

As main conclusion, CFD tools have provided hydraulic optimization and consequent cost reduction of Gabal-el-Asfar WWTP.

#### References

- [1] H. Zhou, D. Smith. Advanced technologies in water and wastewater treatment, *J. Environ. Eng. Sci.*, 1(4) (2002) 247–264.
- [2] Z. Do-Quang, A. Cockx, A. Liné, M. Roustan. Computational fluid dynamics applied to water and wastewater treatment facility modeling, *Environ. Eng. Policy*, 1(3) (1998) 137–147.
- [3] A. Goula, M. Kostoglou, T. Karapantsios, A. Zouboulis. A CFD methodology for the design of sedimentation tanks in potable water treatment: Case study: The influence of a feed flow control baffle, *Chem. Eng. J.* 140 (2008) 110–121.
- [4] C. Knatz, S. Rafferty, A. Delescinskis. Optimization of water treatment plant flow distribution with CFD modeling of an influent channel, *Wat. Quality Res. J Canada*, 50(1) (2015) 72–82.
- [5] J. Bridgeman, B. Jefferson, S.A. Parsons. The development and application of CFD models for water treatment flocculators, *Adv. Eng. Software*, 41(1) (2010) 99–109.
- [6] M. Kostoglou, T. Karapantsios, K.A. Matis. CFD model for the design of large scale flotation tanks for water and wastewater treatment, *Indust. Eng. Chem. Res.*, 46 (2007) 6590–6599.
- [7] J.J. Van der Walt. The modeling of water treatment for process tanks. D. Ing. Dissertation, Rand Afrikaans University Thesis. University of Johannesburg, South Africa, 2002.
- [8] N. Margarit, C. Retana, J. Bacardit, J.J. Malfeito. Optimización del diseño de la PTAR Atotonilco (México) mediante modelización hidráulica, *AEDyR*, 2014.